The new paradigm of an anti-lock braking system for a full electric vehicle: Experimental investigation and benchmarking

Article *in* Proceedings of the Institution of Mechanical Engineers Part D Journal of Automobile Engineering · October 2015

DOI: 10.1177/0954407015608548

CITATIONS
30

READS
4,725

7 authors, including:

Dzmitry Savitski
Technische Universität Ilmenau
66 PUBLICATIONS **675** CITATIONS
SEE PROFILE

Valentin Ivanov
Technische Universität Ilmenau
180 PUBLICATIONS **1,194** CITATIONS
SEE PROFILE

Klaus Augsburg
Technische Universität Ilmenau
153 PUBLICATIONS **827** CITATIONS
SEE PROFILE

Barys Shyrokau
Delft University of Technology
100 PUBLICATIONS **843** CITATIONS
SEE PROFILE

THE NEW PARADIGM OF ANTI-LOCK BRAKING SYSTEM FOR FULL ELECTRIC VEHICLE: EXPERIMENTAL INVESTIGATION AND BENCHMARKING

Dzmitry Savitski [1], Valentin Ivanov[1*], Klaus Augsburg[1], Barys Shyrokau[2], Robert Wragge-Morley[3], Thomas Pütz[4], Phil Barber[5]

[1]Ilmenau University of Technology, Germany

[2]Delft University of Technology, the Netherlands

[3]University of Bristol, United Kingdom

[4]TRW Automotive, Germany

[5]Jaguar Land Rover, United Kingdom

* Corresponding author: Automotive Engineering Group, Ilmenau University of Technology, 98693 Ilmenau, Germany. email: valentin.ivanov@tu-ilmenau.de

ABSTRACT

The presented study discussed developments in the area of anti-lock braking control for full electric vehicles. The main contribution of the paper is the development and experimental validation of the combined electric and hydraulic brake system with application of continuous ABS, which is expected to be more effective in comparison to the existing industrial solutions. It covers the topic of high performance braking and driving comfort under direct slip control function. The research is related to the full electric sport utility vehicle equipped with four individual on-board motors and decoupled electro-hydraulic brake system. The brake controller architecture includes functions of continuous ABS strategy, brake blending algorithm aimed at the minimization of friction brake torque, and operational limitations of electric brakes. The developed brake controller was subjected to different validation procedures, but within the framework of this paper the emergency braking tests on the wet surface with low coefficient of friction are considered. The obtained results demonstrate significant improvements in braking performance, driving comfort and control performance for the electric vehicle continuous ABS control as

compared with diverse vehicle configurations, in particular, with the sport utility vehicle of the same type equipped with internal combustion engine and conventional hydraulic brake system.

Keywords: anti-lock braking system, direct wheel slip control, full electric vehicle, on-board motors, regenerative braking

1 INTRODUCTION

According to the European Commission report [1] CO_2 emissions have to be reduced in the year 2020 to 95 g CO_2/km for the passenger cars that means 32% less emissions compared to the level of the year 2008. Among other factors, such restrictions have motivated in recent years a more intensive development of energy efficient, environment friendly vehicles, in particular, using purely electric propulsion systems. This trend is confirmed by the continuous increase the serial full electric vehicles (FEV) available on the market. Besides improved energy efficiency [2, 3] the electric propulsion can have extra advantages from the viewpoint of fun-to-drive, driving comfort and vehicle safety, especially in the case of individually-controlled motors per each wheel as it is indicated in [4, 5, 6]. Such benefits are possible due to more agile dynamics and higher bandwidth of electric motors as compared with internal combustion engines and hydraulic brake systems used as conventional actuators of wheel torque.

Of particular interest is the operation of electric motors in the generator mode, when the motors carry out a braking function with simultaneous recuperation of vehicle energy released at the service or ABS braking [7, 8]. In the case of the vehicle architecture with individually-controlled electric motors, the anti-lock braking functions can be realized either with pure electric motor operation or as blended actuation of electric motors and friction brakes. The analysis of different ABS principles for electric vehicles is investigated in the presented paper. The recent literature survey [9] performed by authors shows that

although the topic of the ABS control in electric vehicles with individually-controlled electric motors has been discussed in a number of research works providing simulation results [10], but there is a lack of experimental studies on the real vehicle prototypes. Most of published ABS algorithms for electric vehicles have been tested using the model-, software- or hardware-in-the-loop (MiL/SiL/HiL) techniques only. Nevertheless, several publications from automotive original equipment manufacturers (OEM), presenting results of electric vehicle ABS experiments on full-scale vehicle demonstrators in real conditions, give sound arguments in favour of electric motor actuation in a braking mode. For instance, the works [11, 12] has demonstrated that it is possible to reduce braking distance up to 7% on the icy road with regenerative ABS in comparison with conventional hydraulic brake system. The obtained results are related to the Toyota's full electric vehicle with mass of 2100 kg and maximal velocity of 200 km/h. This vehicle is equipped with individual in-wheel electric motors, which can produce wheel torque of 550 Nm with maximal wheel power of 40 kW. Besides the braking efficiency improvement, such brake and propulsion systems layout is also beneficial for the acceleration dynamics involving traction control and can perform functions of active pitch and ride control as well [13]. Another electric vehicle prototype developed by Siemens [14, 15] and known as Roading Roadster Electric (1250 kg) is equipped with two individual electric motors implemented directly in the wheel hub. The Slip Control Boost (SCB) system on this vehicle is actuating friction brakes on the front axle and pure electric brakes are used on the rear axle. This study demonstrates opportunities in energy recuperation and, in particular, represents cases of the pure electric ABS operation on the rear axle. Similar evaluations of the electric motor applicability for ABS were performed in the framework of the project E-VECTOORC [16, 17] for the Range Rover Evoque. Previously published materials demonstrate advantages in use of the continuous ABS [18] with on-board electric motors and confirmed its robustness in different driving conditions [19]. In particular, the experimental tests were performed in transient conditions from low- to high-μ and vice versa [20].

The main goal of the presented study was to explore further the potential of the electric brakes as ABS actuators and to investigate full range of advancements in *braking performance*, *driving comfort* and *control performance* during the ABS braking using on-board electric motors close to their physical limits. It is implicated regarding the physical limits that the on-board electric motors can operate in the frequency domain over 10 Hz that is higher than actuation dynamics of conventional hydraulic anti-lock braking systems. The original regenerative ABS architecture, presented in next sections, is developed for the full electric sport utility vehicle (SUV) with 4 individual on-board motors. For the benchmarking purposes, the same SUV platform with the internal combustion engine (ICE) and the hydraulic brake system is used. The performed analysis includes the comparison of rule-based and continuous ABS control strategies. The corresponding hardware realization of different ABS configurations includes conventional hydraulic, decoupled electro-hydraulic and combined friction and electric brake systems. The main contribution of the paper is the development and experimental validation of the combined electric and hydraulic brake system with application of continuous ABS, which is expected to be more effective in comparison to the existing industrial solutions.

The paper is organized as follows. Firstly, the technical information about the full electric SUV and SUV with ICE is introduced. Then the base braking and ABS modes of all involved types of the brake systems are described and the control logic of the implemented ABS algorithms is explained for each case. Numerical assessment criteria to evaluate braking performance, driving comfort and control performance are proposed. The description of experimental procedure and testing conditions is supplemented with the comparative analysis of the obtained testing results. The paper is finalized with concluding section demonstrating benefits of electric motors for the ABS control.

2 VEHICLE DEMONSTRATOR SPECIFICATIONS

Vehicles for benchmarking. Two Range Rover Evoque SUVs were involved in the testing session to derive benchmarking results. They are represented by full electric vehicle prototype and serial vehicle with ICE. These vehicles are equipped with combined electric and friction brakes and conventional hydraulic brake system respectively. The detailed technical specification of both vehicles is represented below.

Electric vehicle with four on-board individual motors. The full electric SUV prototype was developed in the framework of European project E-VECTOORC [21]. This vehicle has a mass of 2117 kg and is equipped with four electric on-board motors mounted individually at each wheel, Figure 1-3. The electric motors are connected to the wheels through the half-shafts (torsional stiffness of 6500 Nm/rad) and are able to provide the peak torque and power of 200 Nm and 100 kW (for max. 30 sec) respectively. The nominal torque and power are 80 Nm and 35 kW correspondingly. The maximum speed is 15000 rpm. The single-speed gearbox at each motor has a crawl ratio of 1:10.5 to achieve required traction and braking torque. On-board electric systems are supplied with the 600V DC battery, which consists of 15 modules. Each module is represented by 12 lithium-titanate oxide anode cells. The battery has a mass of 274 kg and the total capacity of 9kWh. The dSPACE AutoBox platform is used to control vehicle subsystems and to receive the information from sensors. The platform is directly connected via CAN Bus with the vehicle ECU (electronic control unit), the decoupled electro-hydraulic brake system and the controller of electric motors. The developed control functions (e.g. brake blending, direct slip control, direct yaw control etc.) are flashed on the processing board DS1005.

Figure 1: Vehicle demonstrator with decoupled brake system and four on-board individual electric motors

Figure 2: Decoupled electro-hydraulic brake system mounted on the electric vehicle

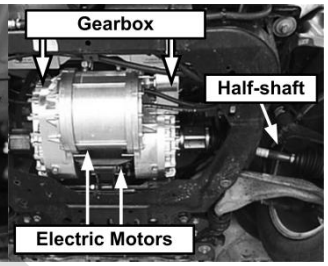

Figure 3: Individual switch reluctance electric motors with gearbox

Conventional vehicle with internal combustion engine. The vehicle with ICE (the 2.0 liters OHC engine) is the Range Rover Evoque equipped with a 6 speed automatic transmission, 245/45 R20 tyres, and a conventional hydraulic serial brake system. The data acquisition is realized with the dSPACE MicroAutoBox via CAN Bus protocol. It allows to collect data both from standard vehicle sensors and supplementary measuring devices, such as extra mounted GPS sensor.

3 BRAKE SYSTEM DESIGN

The proposed study involves three brake system types for the comparative analysis: (i) the conventional hydraulic brake system installed on ICE vehicle; (ii) the decoupled electro-hydraulic brake system installed on the electric vehicle; (iii) the electric motors operating in the generator mode during the braking of the electric vehicle. The configurations (ii) and (iii) give a possibility to analyse both systems in stand-alone mode or in combined operation, where brake torque is distributed between friction brakes and electric motors in accordance with the blending algorithm. Technical specifications of the systems and their operation in the base braking and ABS modes are explained in this section.

Conventional hydraulic brake system, Figure 4, consists of i) brake pedal, ii) brake booster, iii) master cylinder, iv) reservoir with brake fluid, v) hydraulic control unit, vi) friction brakes, vii) solenoid valves, and viii) low pressure accumulator. In the *base-brake mode*, all the valves in the hydraulic modulator are in the initial position. The pressure in callipers is built up directly from the hydraulic coupling with brake pedal. The brake pedal effort is amplified by the vacuum booster and transferred to the master cylinder piston. Thus the pressure in wheel callipers is equal in this state to the base-brake pressure in the master cylinder. The system has a diagonal split, where the one circuit of the master cylinder supplies pressure to left front and rear right callipers; another circuit provides pressure in right front and left rear callipers. In the *ABS mode*, the wheel slip is controlled by a modulation of the brake pressure in the corresponding callipers. A typical control scheme consists of three pressure modulation phases: *apply*, *dump* and *hold*. During the apply phase the base brake pressure from the master cylinder is built up in callipers by opening inlet valve and closing the outlet valve. To unlock wheels and dump the pressure in callipers, the electronic control unit (ECU) opens the outlet valve and closes the inlet valve. The excessive pressure in the case of closed inlet valves is temporary stored in the low pressure accumulator before the pumps can turn it to the reservoir. During the hold phase, the pressure in the callipers is kept constant and both the inlet and outlet valves are closed.

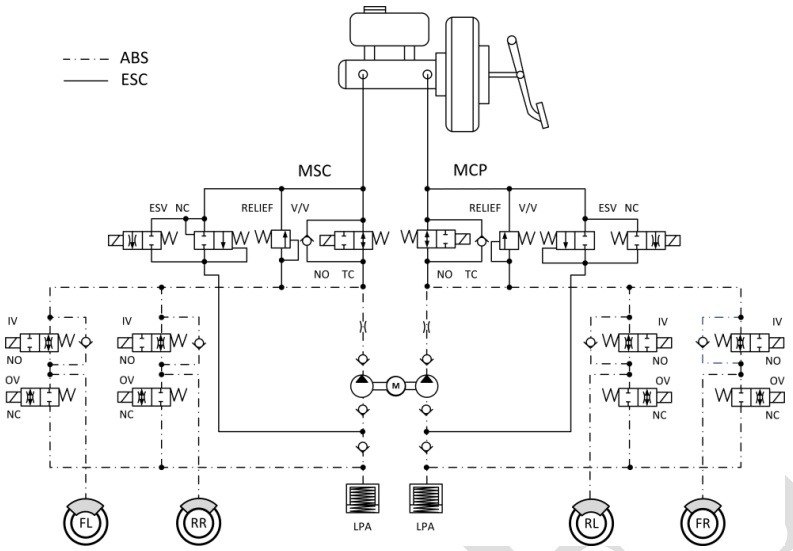

Figure 4: Scheme of conventional brake system
IV – inlet valve; OV – outlet valve; NO – normal open solenoid valve; NC – normal closed solenoid valve; M – electric motor; LPA – low pressure accumulator; MCP – master cylinder primary; MCS – master cylinder secondary.

Decoupled electro-hydraulic brake system. The decoupled electro-hydraulic brake system implemented on the full electric vehicle demonstrator is schematically depicted in Figure 5. In the *base-brake mode* the driver's demand is measured by the pedal travel sensor transmitting the signal to the electro-hydraulic control unit (EHCU). The control of the demanded pressure is performed according to (i) the feedback signal from the pressure sensor mounted before the base-brake valve and (ii) estimated pressures in the callipers. To provide an agile system response, the high pressure accumulator (HPA) charges the pressure up to 180 bar. The boost valve controls proportionally the fluid from HPA to increase the brake pressure or to return it to the reservoir. To provide the force feedback to the driver, the pedal simulator develops the pressure in the master cylinder primary circuit.

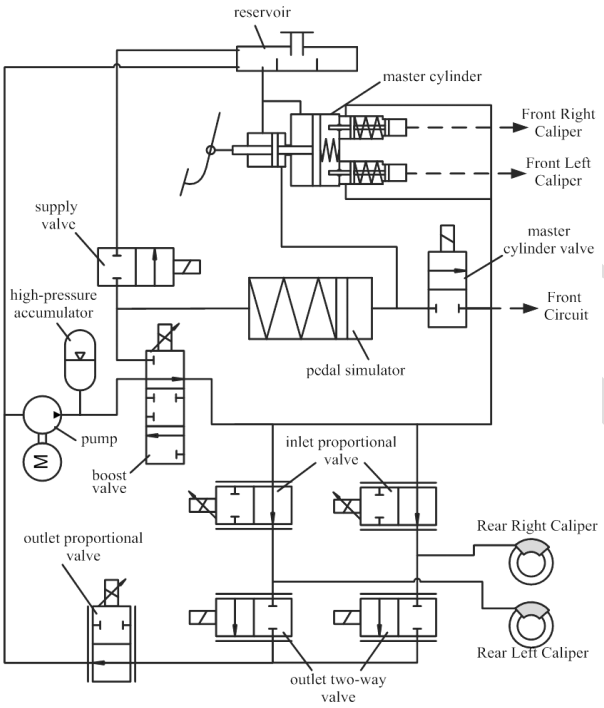

Figure 5: Scheme of decoupled electro-hydraulic brake system, a half view

In the *ABS mode* the inlet valves isolate the boost valve pressure from the callipers when the wheel slipping is detected. In the case all four inlet valves are closed, the operation compliance accumulator causes necessary displacement of the boost valve to prevent the pressure feedback from the dead headed hydraulic circuit. The desired pressure in each calliper is achieved by energizing the proportional inlet and two-way outlet valves.

Electric brake system with on-board motors. The brake system mounted on the full electric vehicle demonstrator consists of the decoupled electro-hydraulic brake system described above and the individual on-board electric motors. The braking torque generated by the electric motors can achieve 2000 Nm in the peak mode, considering the ratio of the gearbox. During the braking maneuver the demanded torque is

continuously distributed between the corresponding actuators. In the proposed system architecture, where the torque is delivered to the wheel through the set of transmission elements, undesirable oscillations are occurring and negatively influencing the driving comfort, durability and control performance. To resolve this issue, an active vibration controller is proposed and implemented [22].

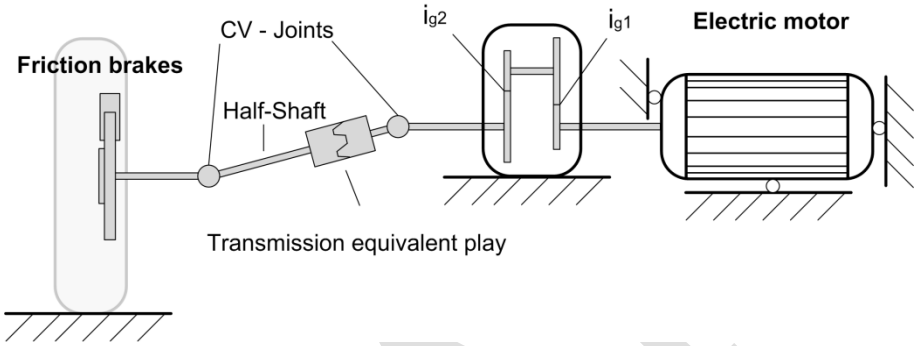

Figure 6: Combined electric and friction brake system

It should be mentioned that electric motors can provide principally new opportunities in ABS control functions because of a wider bandwidth and a quicker system response as compared with conventional friction brakes. Generally, one of the goals of the presented paper is to demonstrate potential benefits of the use of pure electric ABS. Therefore, the brake control algorithm, developed in this study and depicted in Figure 7, is aimed on the maximal utilization of electric motors during braking.

Following Figure 7, the overall torque demand is distributed between the wheels individually according to the developed control algorithm. The torque demand T_{dem} is generated according to the brake pedal travel signal, s_{pedal}. The reactive toque T_{react}, responsible for the direct slip control, is subtracted from the driver's demand and the resulting torque demand further delivered to the Torque limitations and blending functional block. In this part of the controller the demanded torque is saturated according to the predefined control and physical limitations calculating the demand for electric motors T_{em_dem} and friction brakes T_{fric_dem}. In particular, after reaching some certain velocity value (20 km/h in the represented study)

the involvement of the electric motors is progressively decreased replacing them with electric brakes. It is done to hold the vehicle in the stand-still position at zero velocity. Besides that, some physical limitations of the motor and battery are implemented reducing in some specific cases the use of the electric brakes (e.g. when the battery is full). The resulting control demands T_{em_dem} and T_{fric_dem} are further realized by the corresponding actuators.

The State and parameter estimator carries out the identification of parameters which cannot be measured directly but required for some control functions, e.g. slip target adaptation and slip control.

The reactive torque and base brake controller functionality are explained in more details in the Section 4 of the paper.

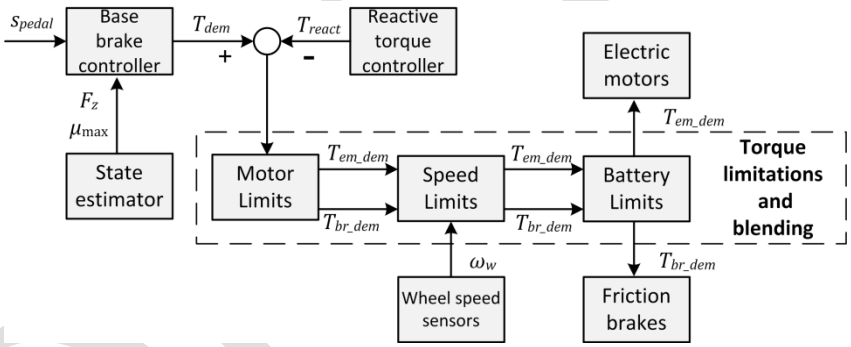

Figure 7: Brake blending control strategy

4 ANTI-LOCK BRAKING SYSTEM ARCHITECTURE

The proposed continuous ABS is specifically developed for combined friction and electric brake system and is characterized by the high operational frequency, which can be supported by the motors and in some range by the electro-hydraulic brake system. To compare the braking performance of the continuous brake control, two alternative rule-based algorithms are analyzed and implemented on the conventional

hydraulic and decoupled electro-hydraulic brake systems. In this section the rule-based and continuous ABS control strategies are explained.

Rule-based control. The rule-based ABS algorithm realizes the pressure modulation with three (*apply*, *dump* and *hold*) phases to control the wheel slip. Nowadays, such control approach is widely used in industry due to its high robustness and relatively low demands to the control units. Considering the selected control strategies and some deviations in the calliper pressure estimation, an operation of the ABS outside the extremum area of the μ-s diagram is inevitable. The principles of the wheel slip control can be explained as follows. The ABS is being activated as soon as the wheel reaches a certain wheel slip threshold. To reduce the wheel slip through acceleration of the wheel, the pressure in the corresponding brake calliper is being released until the system state, where certain control thresholds in relation to the wheel slip value or acceleration are achieved. After that the pressure can be increased again. The frequency of these control loops is about 1–3 Hz as long as significant deviations between the actual and reference wheel speed occur.

The ABS reference slip depends on the current road conditions. It is based on the slip gradient in the case of high-μ surface and it is defined by the estimated peak slip of the road surface. The slip calculation is closely related to the measurements of the vehicle velocity. Here some inaccuracies can occur considering the fact that the velocity is estimated by indirect methods. The inaccuracy in the velocity estimation has negative on the ABS performance.

In this study the different modifications of the rule-based ABS algorithm are realized by the conventional hydraulic and decoupled electro-hydraulic brake systems. These algorithms and systems are implemented by two different brake system manufacturers.

Continuous ABS control. Continuous ABS control strategy does not switch between the defined states in comparison to the known rule-based approaches but continuously modulates the pressure in callipers according to the calculated control error [23]. Such approach has not found wide application in the industry yet. The continuous approach demonstrates also better wheel slip tracking and reduced number of tuning parameters but can suffer from the insufficient robustness that depends on the selected control law (PID, sliding mode control, *etc.*).

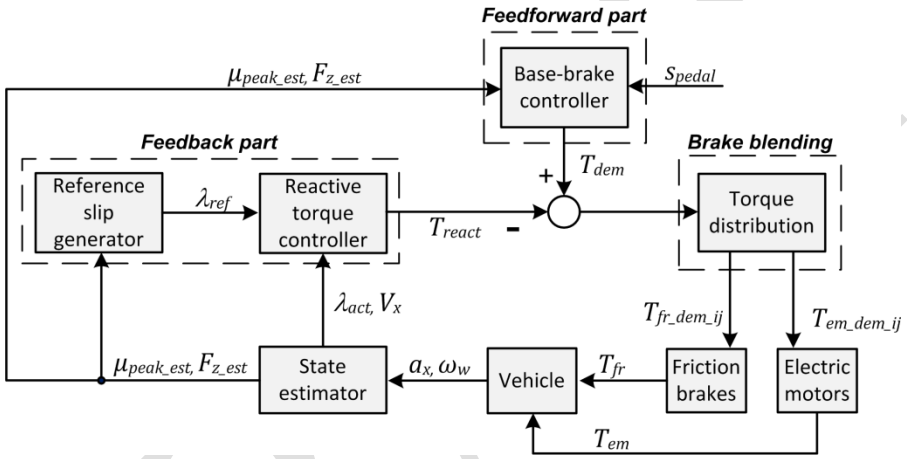

Figure 8: Scheme of electric anti-lock braking system control

The control strategy applied to the combined electric and friction brake system is schematically illustrated in Figure 8. The ABS is activated after reaching certain slip ratio thresholds. To derive the demanded vehicle braking torque the sensor measuring brake pedal travel s_{pedal} is utilized. Using this signal the Base Brake Controller calculates the overall brake torque demand T_{dem}. This operation is performed involving predefined relation between brake pedal travel and demanded vehicle acceleration. In terms to avoid some excessive torque demand the predictive torque T_{pred} is computed in the Base Brake Controller. The predictive torque is considered as the feedforward part of the slip controller and can be expressed as follows:

$$T_{pred} = \mu_{\max} F_z r + k_{pred} \left(\mu_{\max} F_z r \right), \quad (1)$$

where μ_{max} is the estimated value of maximum friction coefficient, F_z is the estimated normal wheel load, r is the tire rolling radius, k_{pred} is the correction coefficient.

To keep the wheel slip at certain threshold λ_{ref}, the Reactive torque controller generates the torque T_{react} which is further subtracted from the overall torque demand T_{dem}. The resulting torque demand is further distributed between the friction T_{fr_dem} and electric brakes T_{em_dem} as it was mentioned in Section 3 of the paper and depicted in the Figure 7.

The reactive torque controller function is based on the estimation of the actual wheel slip ratio λ_{act} and the desired/reference slip ratio λ_{ref} derived from the Reference slip generator.

To receive the similar behaviour of the system independently from its velocity, the vehicle velocity is estimated and used for gain scheduling in the reactive torque controller. The estimation of the velocity is performed using the method based on the Kalman filter with scheduled covariance matrices proposed in [24]. The generation of the reference value of the wheel slip is based on the estimated values of the vertical wheel load F_z and the peak value of the road friction coefficient of friction μ_{peak_est}. The corresponding state variables are derived in the state estimation block by the indirect methods (this is not discussed in the proposed paper).

The reactive torque is generated according to the equation:

$$T_{react} = \nu_{PI} \cdot \xi_{driver\_dem}, \quad (2)$$

where ξ_{driver_dem} is the correction factor, which saturates the reactive torque in order to prevent generation of the wrong torque values and considers the driver demand. The generation of the reactive torque is based on the PI-control law:

$$\nu_{PI} = \left(\nu_P + \nu_I \right). \quad (3)$$

To analyse the influence of the gains and vehicle velocity on the system frequency response a quarter car model was used in the closed loop configuration. Vehicle and wheel dynamics can be represented as follows:

$$m\dot{V}_x = -F_x\,, \tag{4}$$

$$J\dot{\omega} = rF_x - T_w sign(\omega)\,, \tag{5}$$

where m is the vehicle mass, r is the tire rolling radius, and F_x is the longitudinal force, which has been calculated in the presented analysis on the basis of the Burckhardt tire model (Burckhardt, 1993) as function of the wheel slip λ and the maximum tire road friction coefficient μ_{road}:

$$F_x = F_z \mu(\lambda, \mu_{road})\,. \tag{6}$$

From Eqs. (4-6) the actual slip can be derived:

$$\dot{\lambda} = -\frac{1}{V_x}\left(\frac{1}{m}(1-\lambda) + \frac{r^2}{J}\right)F_z \mu(s, \mu_{road}) + \frac{1}{V_x}\frac{r}{J}T_w\,, \tag{7}$$

where J is the wheel mass moment of inertia.

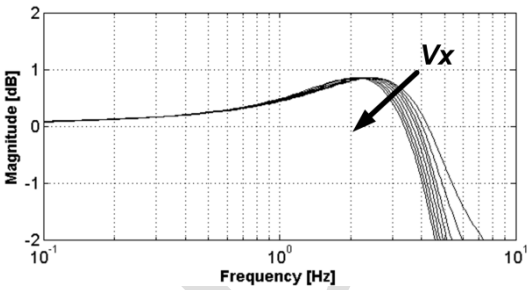

Figure 9: Systems frequency response according to the vehicle velocity variation.

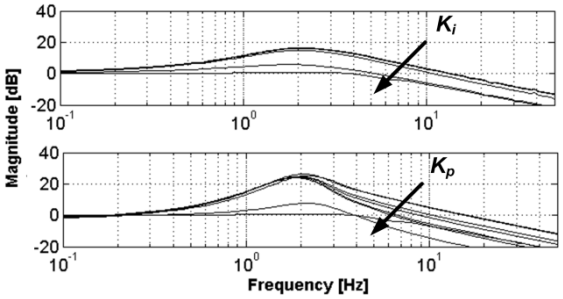

Figure 10: Systems frequency response according to the gains variation.

As it can be seen in Figure 9 vehicle velocity variation certainly influences on the system response characterisitics. Therefore, the proportional gain is scheduled according to the vehicle velocity to derive the predictable system behavior independently from this state variable:

$$v_P = K_P(V_x)\min(0,e). \tag{8}$$

where e is the control error.

The integral gain is scheduled in a similar way with use of the anti-windup part:

$$\dot{v}_I = K_I(V_x, mode)\min(0,e) - \alpha \dot{T}_{dem\_wheel} sat(e) v_I, \tag{9}$$

where coefficient α is related to the anti-windup part and determines how quick the integral part should be reduced, *mode* determines the driving mode.

The saturation of the control error is realized as follows:

$$sat(e) = \begin{cases} 1, & \max(0,e) > v_e \\ e, & \max(0,e) < v_e \end{cases}, \tag{10}$$

where v_e is a saturation variable, function *max(0,e)* selects the maximal value between zero and control error e.

The influence of the gains variation on the system response is represented on Figure 10. In terms to achieve required system behavior the optimization procedure of PI-gains was performed using the IPG CarMaker simulator. The formulated cost-function includes stopping distance s_{dist}, integral of time-multiplied absolute value of error (ITAE) and root mean square error (RMSE) of the wheel slip λ_{ij}:

$$J = \left(w_1 \frac{s_{dist}}{s_{dist,ref}} + w_2 \frac{\sum ITAE(\lambda_{ij})}{\max\left(\sum ITAE(\lambda_{ij})\right)} + w_3 \frac{\sum RMSE(\lambda_{ij})}{\max\left(\sum RMSE(\lambda_{ij})\right)} \right) \tag{11}$$

where w_i is the weighting factor, λ_{ij} is the wheel slip ratio of the corresponding wheel (i={*front;rear*}; j={*left; right*}). The reference values in denominator for each of the parameters where determined specifically in each test. The tests are represented by straight-line braking maneuvers with different initial vehicle velocity. In such way the optimal values of the PI-gains have been derived in simulation. For this purpose the Differential Evolution optimization strategy was applied.

5 EXPERIMENTAL RESULTS

Manoeuvre description. All the experiments were carried out on the inhomogeneous road with the low coefficient of friction at the Ford Lommel Proving Ground [25]. The road is composed of the polished basalt tiles, which are continuously wetted by the sprinklers, Figure 11. For all testing cases the emergency braking (high brake pedal velocity) is investigated with initial vehicle speed of 60 km/h.

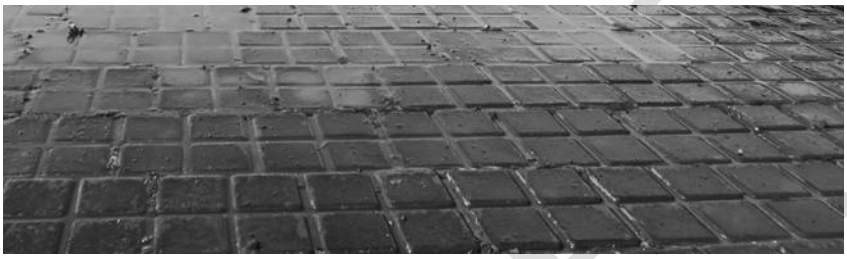

Figure 11: Road surface

Assessment criteria. To evaluate the overall performance of the different ABS control strategies and corresponding brake systems architectures, the *braking performance*, *ABS control performance* and *driving comfort* are investigated and corresponding quantitative criteria were formulated. The numerical data, experimentally obtained for all criteria, are represented in the Table 1 before the conclusions.

Braking performance. The main purpose of the ABS is to achieve a required vehicle deceleration in the conditions, where the wheels are tending to lock. The vehicle deceleration profile for the four investigated cases is displayed on Figure 12. Here the rule-based ABS strategy implemented on the hydraulic and electro-hydraulic brake systems demonstrates comparable results in terms of the braking time and the average deceleration of 1.43 and 1.44 m/s^2 respectively. The highest achieved deceleration (1.87 m/s^2) is realized by the continuous ABS system, which involves electric brakes most of the operation time.

In terms to assess the effect of the ABS operation, the index of performance can be considered. It shows the relation between the deceleration of the vehicle with and without ABS activation [26]:

$$ABSIP = a_{ABS} / a_{skid} \quad . \tag{6}$$

This relative criterion is also comparable for the rule-based ABS on conventional hydraulic and decoupled electro-hydraulic systems (1.40 and 1.34 respectively) and confirms more beneficial use of the continuous ABS with combined brake system (*ABSIP=1.74*).

Driving comfort during braking. Some negative influence on the driver perception during the ABS braking occurs due to the fluctuations in the realized brake force, which produce oscillations in the vehicle deceleration. To characterize the driving comfort characteristics, the vehicle jerk signal is derived, Figure 13. The less is the vehicle jerk the better comfort characteristics are provided by the ABS. For the quantitative comparison of the driving comfort it is proposed to take the integral of time-multiplied absolute value of error ITAE of vehicle jerk with desired value of zero:

$$I_{\lambda_{ij}} = \int_{t_1}^{t_2} |j_x| \cdot t dt \tag{7}$$

The lowest ITAE value has been obtained for the braking with continuous ABS of electric vehicle (2.92 m/s^2) as compared with the ABS of conventional vehicle (5.36 m/s^2) and decoupled electro-hydraulic ABS (12.00 m/s^2). Therefore the developed continuous ABS strategy is certainly advantageous also from viewpoint of jerk-related driving comfort.

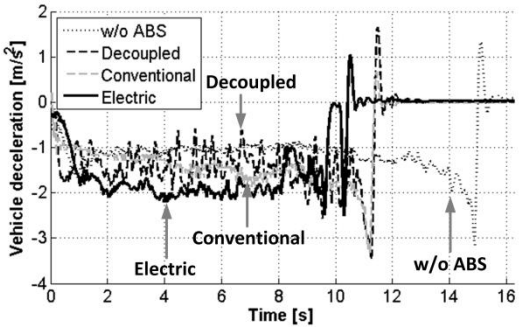

Figure 12: Vehicle deceleration

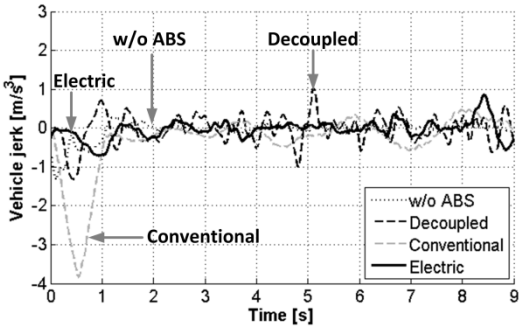

Figure 13: Vehicle jerk

System adaptability. The important factor of the ABS performance is how agile system reacts on the wheel slip dynamics. To assess this agility quantitatively the peak value of the initial ABS control cycle can be numerically evaluated and expressed in percent:

$$\omega_{peak} = \frac{\omega_{\max} - \omega_{\min}}{\omega_{\max}} \cdot 100\% \tag{8}$$

The evaluated peak values for the initial ABS control cycle can be also clearly seen on the graphs of the vehicle and wheel velocity, Figure 14. As soon as on the electric vehicle electro-hydraulic brake system was mostly used as the backup solution, tuning of the system was not performed. Due to this fact the ABS of the decoupled electro-hydraulic brake system has a peak of 57% and 31% for front and rear wheels, which can be significantly reduced by adjusting the control parameters of the algorithm. A quicker reaction is observed by the conventional hydraulic ABS: peak value of 36% both on front and rear wheels. The best performance in terms of the system adaptability and reaction is demonstrated the developed continuous ABS implemented on the combined brake system, where peak values of the initial cycle are just of 6% and 8% for front and rear wheels respectively.

Wheel slip ratio. As soon as the rule-based algorithms and both hydraulic and electro-hydraulic brake systems are represented by the industrial solutions, the reference value of the wheel slip ratio cannot be derived and tracking performance of the system cannot be analysed for these two systems. For the case of continuous ABS, where the reference value of the slip ratio was available, it can be clearly seen on Figure 15 how precise the system keeps the wheel slip ratio around the reference value as differentiated from the typical operation of the rule-based approaches and hydraulic systems.

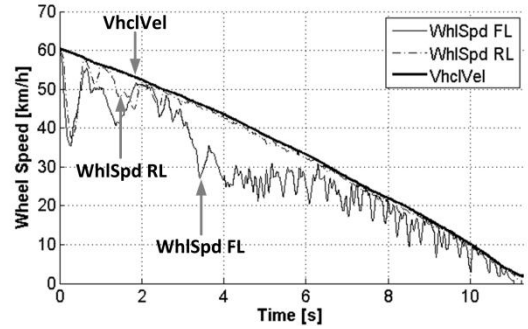

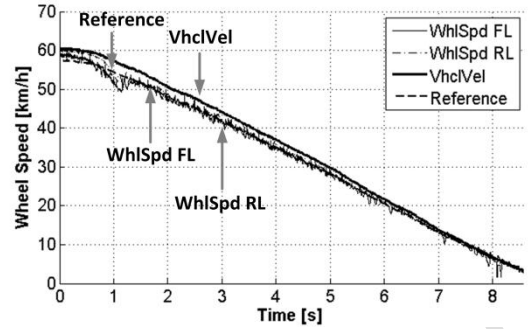

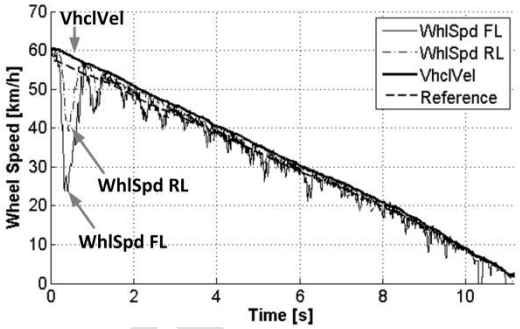

Figure 14: Wheel and vehicle speeds
Upper left – conventional hydraulic; upper right – decoupled electro-hydraulic; bottom left – combined electric and friction brakes

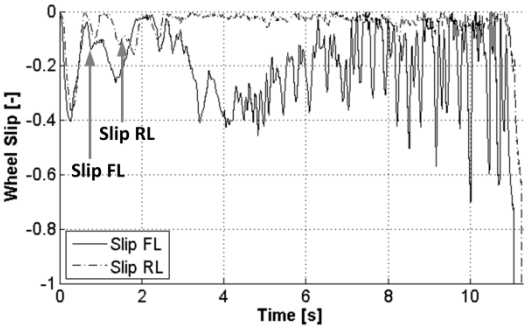

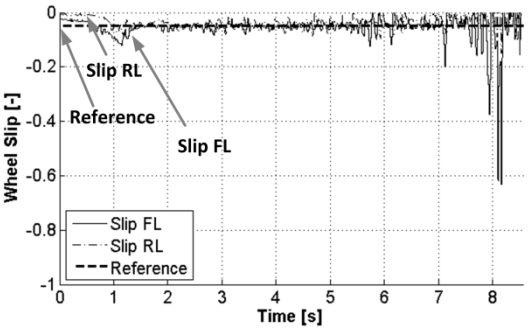

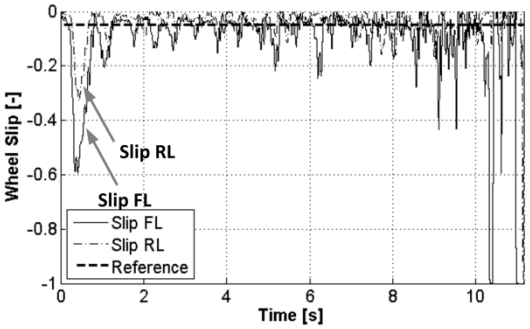

Figure 15: Wheel slip during the ABS braking
Upper left – conventional hydraulic; upper right – decoupled electro-hydraulic; bottom left – combined electric and friction brakes

Actuator operation. The operation of rule-based algorithms is characterized first of all by the limitations in the ABS frequency, which reaches only 1-3 Hz (Figure 16) in particular cases. Considering the algorithm switching between different system states, a suboptimal operation of the ABS is inevitable for such algorithms.

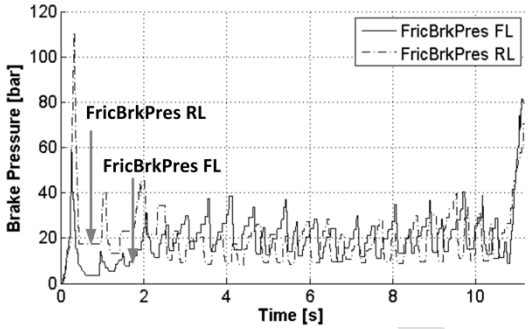

Figure 16: Decoupled electro-hydraulic brake system pressure

For continuous ABS, the required torque demand most of the time was realized by the electric brake system, Figure 17, and the decoupled electro-hydraulic brake system is gradually involved in the braking process only to the end of braking process, Figure 18. As it can be seen on the Figure 17, operational frequencies can achieve 8-10 Hz in this case that is distinctly higher than in the case of conventional brake systems.

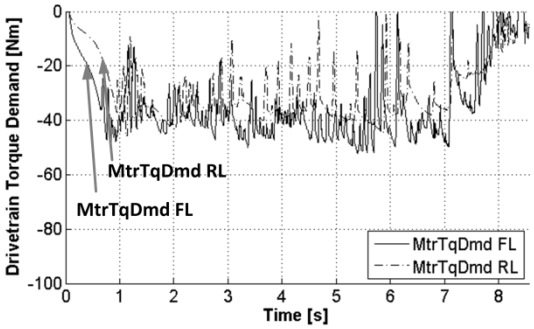

Figure 17: Electric brake system torque demand during ABS braking

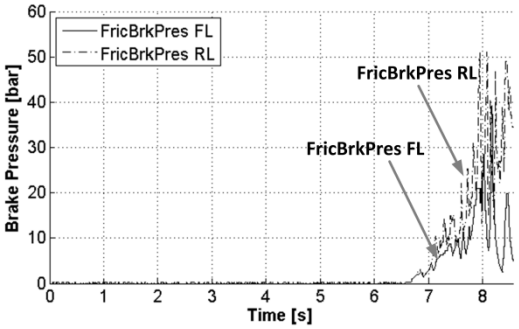

Figure 18: Hydraulic brake system pressure during ABS braking

Quantitative evaluation. The proposed quantitative criteria are summarized in the Table 1. They are also normalized in terms to provide comparison in percent and represented on Figure 19. Here the value of 100% corresponds to the best performance.

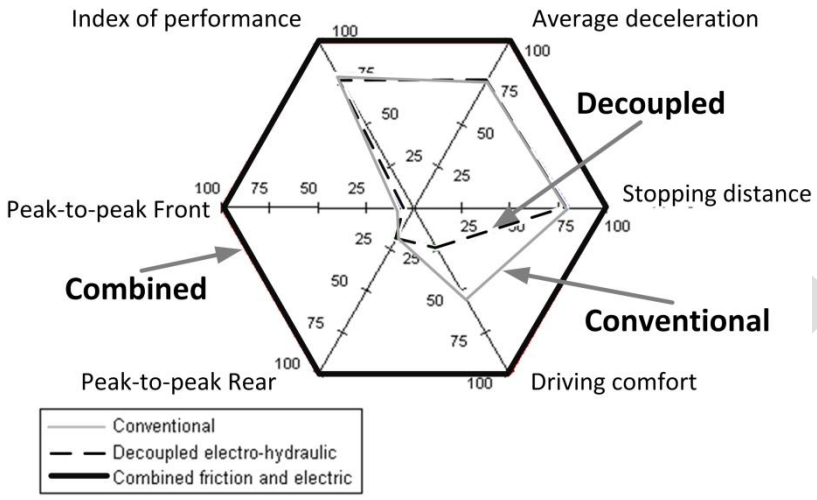

Figure 19: Anti-lock braking system benchmarking diagram

Summarizing aforementioned analysis and numerical data it is possible to claim that:

- Braking distance of continuous electric ABS is 20% less than in case of rule-based ABS;
- In terms of the control performance the electric ABS showed reduction of the peak-to-peak value from 75% up to 90% in comparison to the other investigated solutions;
- Better driving comfort was achieved in the case of electric ABS by reduction of the vehicle jerk up to 76% as compared with the rule-based systems.

Table 1 – Quantitative benchmarking criteria

Criterion / Type	Braking performance			ABS control performance				Driving comfort
	Brake distance, m	**Average deceleration, m/s²**	**Index of performance**	**Average slip, %**		**Peak to peak value, %**		**Jerk ITAE, m/s²**
Conventional	100.2	1.43	1.40	*FL*	24	*F*	36	5.36
				FR	23			
				RL	8	*R*	36	
				RR	20			
Decoupled electro-hydraulic	100.7	1.44	1.34	*FL*	14	*F*	57	12.00
				FR	14			
				RL	8	*R*	31	
				RR	9			
Combined friction and electric	80.7	1.87	1.74	*FL*	14	*F*	6	2.92
				FR	14			
				RL	10	*R*	8	
				RR	10			

5 CONCLUSIONS

From the performed analysis and previous published studies in the area of regenerative braking it is clearly seen that potential of the electric brakes was still underestimated. It relates especially to the case of ABS braking where safety, energy efficiency and driving comfort can be significantly improved. It particular, the introduced experimental results have demonstrated that the operation of electric brakes close to their physical limits provides a feasible effect in braking performance: around 20% of braking distance reduction can be achieved in comparison to the existing and prototypical industrial solutions.

Besides this important fact, the continuous electric ABS provides the agile operation significantly reducing the wheel velocity peak-to-peak value of initial cycle. It demonstrates special benefits and possible improvements in the system adaptability and control performance.

Moreover, recognizable enhancements in driving comfort are achieved by reduction of wheel force fluctuations during the ABS braking. Such approach as consequence positively influences on the driving perception reducing the vehicle jerk. Compared to other systems the operation of continuous ABS shows reduction from 46% up to 76% in ITAE of the vehicle jerk.

ACKNOWLEDGEMENTS

The authors are grateful for the support of other members of the E-VECTOORC project consortium. The research leading to these results has received funding from the European Union Seventh Framework Program FP7/2007-2013 under grant agreement no. 284708.

REFERENCES

1. Sharpe R and Smokers R. Assessment with respect to long term CO2 emission targets for passenger cars and vans. *Report to European Commission*, 2009.
2. Zhang J, Lv C, Gou J and Kong D. Cooperative control of regenerative braking and hydraulic braking of an electrified passenger car. Proceedings of the Institution of Mechanical Engineers Part D: Journal of Automobile Engineering 2012, 226(10): 1289–1302.
3. Yin G and Jin X. Cooperative control of regenerative braking and antilock braking for a hybrid electric vehicle. Mathematical Problems in Engineering 2013, 890427: 1-9.
4. De Novellis L, Sorniotti A, Gruber P and Pennycott A. Comparison of Feedback Control Techniques for Torque-Vectoring Control of Fully Electric Vehicles. *IEEE Transactions on Vehicular Technology* 2014; 63(8): 3612-3623.
5. De Novellis L, Sorniotti A and Gruber P. Design and comparison of the handling performance of different electric vehicle layouts. *Proceedings of the Institution of Mechanical Engineers: Part D-Journal of Automobile Engineering* 2013; 228: 218-232.

6. Pennycott A, De Novellis L, Sabbatini A, Gruber P and Sorniotti A. Reducing the Motor Power Losses of a Four-Wheel Drive Fully Electric Vehicle via Wheel Torque Allocation. Proceedings of the Institution of Mechanical Engineers: Part D-Journal of Automobile Engineering 2014, 228(7): 830-839.

7. Oleksowicz S, Burnham K, Phillip N, Barber P, Curry E and Grzegozek W. Regenerative Braking Control for High Level Deceleration on Low Mu Surface. SAE Int. J. Alt. Power. 2015, 4(1):209-224.

8. Oleksowicz S, Burnham K, Barber P, Toth-Antal B, Waite G, Hardwick G, Harrington C and Chapman J. Investigation of regenerative and anti-lock braking interaction, International Journal of Automotive Technology 2013, 14(4), 641-650.

9. Ivanov V, Savitski D and Shyrokau B. A Survey of Traction Control and Anti-lock Braking Systems of Full Electric Vehicles with Individually-Controlled Electric Motors. *IEEE Transactions on Vehicular Technology* 2015, PP(99): 1-20.

10. Song C, Wang J and Jin L. Study on the composite ABS control of vehicles with four electric wheels. Journal of Computers 2011, 6(3): 618-626.11. Murata S. Innovation by in-wheel-motor drive unit. *Vehicle System Dynamics: International Journal of Vehicle Mechanics and Mobility* 2012, 50(6): 807-830.

12. Akaho D, Nakatsu M, Katsuyama E, Takakuwa K and Yoshizue K. Development of vehicle dynamics control system for in-wheel-motor vehicle. *in Proc. JSAE Annual Congress (Spring)*, Yokohama, Japan, 2010.

13. Savitski D, Augsburg K and Ivanov V. Enhancement of energy efficiency, vehicle safety and ride comfort for all-wheel drive full electric vehicles. *in Proc. EuroBrake*, Lille, France, 2014.

14. Freitag G, Gerlich M, Bergmann D, Pais G and Fischer B. Replacement of the friction brake by a wheel hub drive. *in Proc. The 3rd International Munich Chassis Symposium chassi.tech plus*, Munich, Germany, 2012.

15. Freitag G, Klopzig M, Schleicher K, Wilke M and Schramm M. High-performance and highly efficient electric wheel hub drive in automotive design. *in Proc. The 3rd International Electric Drives Production Conference (EDPC)*, Nuremberg, Germany, 2013.

16. Ivanov V, Orus J, Pütz T, Brungs F, Savitski D and Shyrokau B. Electric and friction braking control systems for awd electric vehicles. *in Proc. FISITA 2014 World Automotive Congress*, Maastricht, the Netherlands, 2014.

17. Ivanov V, Savitski D, Augsburg K, Knauder B, Barber P and Zehetner J. Wheel Slip Control for All-Wheel Drive Electric Vehicle. *in Proc. The 18th International Conference of the ISTVS 2014*, Seoul, Korea, 2014.

18. Savitski D, Ivanov V, Shyrokau B, De Smet J and Theunissen J. Experimental Study on Continuous ABS Operation in Pure Regenerative Mode for Full Electric Vehicle. *SAE Int. J. Passeng. Cars - Mech. Syst.* 2015, 8(1):364-369.

19. Savitski D, Höpping K, Ivanov V and Augsburg K. Influence of the Tire Inflation Pressure Variation on Braking Efficiency and Driving Comfort of Full Electric Vehicle with Continuous Anti-Lock Braking System. *SAE Technical paper 2015-01-0643*, 2015.

20. Ivanov V, Savitski D, Augsburg K and Barber P. Electric vehicles with individually controlled on-board motors: Revisiting the ABS design. *in Proc. Of IEEE International Conference on Mechatronics (ICM)* 2015, 323-328.

21. www.e-vectoorc.eu, last accessed on 7th February 2015.

22. Rodriguez, J.M., Meneses, R. and Orus, J. Active vibration control for electric vehicle compliant drivetrains. in Proc. *Industrial Electronics Society Conference*, Vienna, Austria, 2013.

23. Ivanov V, Shyrokau B, Savitski D, Orus J, Meneses R, Rodríguez-Fortún JM, Theunissen J and Janssen K. Design and Testing of ABS for Electric Vehicles with Individually Controlled On-Board Motor Drives. *SAE Int J Passeng Cars - Mech Syst* 2014, 7(2):902-913.

24. Kiencke U and Nielsen L. Automotive control systems: For engine, driveline, and vehicle. *Berlin: Springer* 2005, p. 512.

25. www.fordlpg.com, last accessed on 7th February 2015.

26. Marshek K, Cuderman J and Johnson M. Performance of Anti-Lock Braking System Equipped Passenger Vehicles – Part II: Braking as a Function of Initial Vehicle Speed in Braking Maneuver. *SAE Technical Paper 2002-01-0307*, 2002.